Completely L^2 integrable method for strong-coupling multichannel photoionization: Photoelectron emission of He between the $N=3$ and 4 thresholds

F. Martín
Departamento de Química C-14, Universidad Autónoma de Madrid, 28049-Madrid, Spain
(Received 16 February 1993)

We present a completely L^2 integrable method to evaluate continuum states in multichannel photoionization. The Feshbach theory is used to separate the resonant and nonresonant components of the wave function. The nonresonant continuum is built from discretized uncoupled channels, using a formal scattering theory. In practice, the coupling between channels is introduced in a purely algebraic way, by simply solving a system of linear equations. The advantage of the present approach is that it can be used irrespective of the interaction strength between the uncoupled states. We have applied the method to study photoionization of helium between the $N=3$ and 4 thresholds. The results are in good agreement with the existing experimental data.

PACS number(s): 32.80.Fb, 32.80.Dz, 31.50.+w

I. INTRODUCTION

Representation of scattering states by L^2 integrable functions is a topic of continuous interest in atomic physics. Discretization of continuum wave functions avoids numerical solution of (coupled) differential equations, and permits the use of algebraic techniques, which do not require too much computer time. Therefore, use of larger basis sets is feasible, thus yielding a better description of electron correlations.

Discretized wave functions do not satisfy the proper δ-function normalization of continuum states. Although this is not a problem when one performs a summation over the entire continuum spectrum, for a specific energy, the continuum state must be renormalized. Therefore, a discretization technique must not only provide the wave functions, but also the correct renormalization factors.

Many different L^2 methods have been proposed in the literature for the case of a single open channel. On the other hand, when more than one channel is open, the use of L^2 methods is scarce. The reason is that, besides the renormalization problem, one has to satisfy boundary conditions that couple all channels asymptotically. Direct diagonalization of the Hamiltonian with L^2 integrable functions yields couplings that depend on the basis set, so that such a procedure cannot be used in multichannel problems. The solutions proposed in the literature (see, for instance, Refs. [1–14]) make use of the formal scattering theory to ensure the correct boundary conditions. Many of these approaches have been applied to model systems. Very recently, the works of Refs. [8–17] have been successful in applying multichannel discretization to real systems, such as electron-hydrogen scattering [8,9] and helium photoionization [11,13–17].

In previous works [12,14], we have developed an L^2 method that has been applied to study photoionization of helium below $N=3$ from both the ground [13–15] and the first $^{1,3}S^e$ excited states [16,17]. In Ref. [14], hereafter called paper I, we treated resonant and nonresonant components separately by using the Feshbach theory. For the nonresonant part, we used L^2 representations of either the K-matrix equations or the corresponding Green's operator, in a basis of discretized uncoupled continuum states. Both methods ensure the proper δ-function normalization as well as the correct asymptotic behavior of the continuum wave functions. Calculations of the K matrix and the Green's function were done in a perturbative way: in the first case, by solving iteratively the K-matrix equations, and in the second, by using a Born expansion in terms of another Green's operator associated to the uncoupled continua. In the K-matrix calculations, convergence is achieved when interchannel interactions are smaller than energy differences between discretized states, while in the Green's operator expansion, the convergence condition is the usual one for Born series, which is stronger than the previous one. These inherent limitations of perturbative expansions prevent the use of the method proposed in paper I when interchannel coupling is very strong. This is the case for the helium atom above the $N=3$ threshold, the H^- negative ion, and many others.

In this paper, we present an alternative way to calculate continuum wave functions using L^2 bases, which does not present the former restrictions and, therefore, can be used for any system, irrespective of the strength of interchannel coupling. This method is fully algebraic: it involves the solution of systems of linear equations in the complex plane, which can be done with standard techniques.

We have applied the method to the calculation of photoionization cross sections of He between the $N=3$ and 4 thresholds. In this energy region, there are nine open channels $1s\epsilon p$, $2s\epsilon p$, $2p\epsilon s$, $2p\epsilon d$, $3s\epsilon p$, $3p\epsilon s$, $3p\epsilon d$, $3d\epsilon p$, and $3d\epsilon f$, of which the last five ones are strongly coupled. The $4lnl'$ resonances also lie in this energy range. The only calculation of photoionization cross sections of helium above the $N=3$ threshold that we are aware of has been reported by Hayes and Scott [18] using the R-matrix method. On the other hand, there is a number of theoretical works that have provided energy positions

and total autoionization widths for the $4lnl'$ resonances [19–24]. From the experimental side, Woodruff and Samson [25] have measured the total cross sections for leaving the He^+ ion in an excited state ($\sigma_{N=2}+\sigma_{N=3}$) as a function of the photon energy, and Heimann *et al.* [26] have been able to separate the $N=3$ contribution at four different energies. More recently, Domke *et al.* [27] have obtained the spectrum for the total photoionization cross section with high-energy resolution, and Zubek *et al.* [28] have measured the $N=2$ differential cross section at 90°.

The paper is organized as follows. The theoretical method is explained in Sec. II. To be self-contained, we will repeat here some basic equations of paper I that are needed to understand the main features of this approach. In particular, we will pay special attention to the construction of the Green's operator, needed to build the continuum wave function. In Sec. III, we present the calculated cross sections for the photoionization of He between the $N=3$ and 4 thresholds. Presentation of the nine partial cross sections and the resonance parameters is beyond the scope of the present paper and would lengthen it unnecessarily. Instead, we will show the results that are relevant for comparison with the existing experimental and theoretical data, in order to gauge the validity of our method. Complete information on partial cross sections and resonance parameters will be presented in a forthcoming paper. In Sec. III, we also discuss our results. Finally, we end the paper with some conclusions in Sec. IV.

Atomic units are used throughout the paper unless otherwise stated.

II. THEORY

Our method to calculate the continuum wave function is based on the Feshbach theory [29]. The advantage of this theory is that the resonant and nonresonant contributions to the wave functions are handled separately and, therefore, one can use specific methods to calculate each part. As shown in paper I, for each channel μ, the exact eigenfunction $\psi^-_{\mu E}$ of the Hamiltonian $\mathcal{H}$ can be written

$$|\psi^-_{\mu E}\rangle=\frac{\langle\phi_s|Q\mathcal{H}P|P\psi^{0-}_{\mu E}\rangle}{E-\mathcal{E}_s-\Delta_s(E)-i[\Gamma_s(E)/2]}|\phi_s\rangle +[1+G^{(s)}_Q(E)Q\mathcal{H}P]\times\left[|P\psi^{0-}_{\mu E}\rangle+\frac{\langle\phi_s|Q\mathcal{H}P|P\psi^{0-}_{\mu E}\rangle}{E-\mathcal{E}_s-\Delta_s(E)-i[\Gamma_s(E)/2]}\times G^{(s)-}_P(E)P\mathcal{H}Q|\phi_s\rangle\right], \quad (1)$$

where P and Q are orthogonal projection operators satisfying

$$\lim_{r_i\to\infty}P\psi^-_{\mu E}=\psi^-_{\mu E}\ , \quad (2)$$

$$P+Q=1\ , \quad (3)$$

ϕ_s is a resonant wave function which is the solution of a projected Schrödinger equation in the Q subspace:

$$(Q\mathcal{H}Q-\mathcal{E}_n)\phi_n=0\ , \quad (4)$$

$G^{(s)}_Q(E)$ is the Green's operator in Q subspace in which the s state has been excluded:

$$G^{(s)}_Q(E)=\sum_{n\ (\neq s)}\frac{|\phi_n\rangle\langle\phi_n|}{E-\mathcal{E}_n}\ , \quad (5)$$

$P\psi^{0-}_{\mu E}$ is a nonresonant wave function which is the solution of the following Schrödinger equation in P subspace:

$$\left[P\mathcal{H}P+\sum_{n\ (\neq s)}\frac{P\mathcal{H}Q|\phi_n\rangle\langle\phi_n|Q\mathcal{H}P}{E-\mathcal{E}_n}-E\right]P\psi^{0-}_{\mu E} \equiv(\mathcal{H}'-E)P\psi^{0-}_{\mu E}=0\ , \quad (6)$$

$G^{(s)-}_P(E)$ is the corresponding Green operator in P subspace:

$$G^{(s)-}_P(E)=\lim_{\eta\to0}\frac{1}{E-\mathcal{H}'-i\eta}\equiv G^{(s)}_P(E)+i\pi\delta(E-\mathcal{H}')\ , \quad (7)$$

$\Gamma_s(E)$ is an energy-dependent "width"

$$\Gamma_s(E)=\sum_\mu\Gamma^s_\mu(E)=2\pi\sum_\mu|\langle P\psi^{0-}_{\mu E}|P\mathcal{H}Q|\phi_s\rangle|^2\ , \quad (8)$$

and $\Delta_s(E)$ an energy-dependent "shift"

$$\Delta_s(E)=\mathrm{Re}\langle\phi_s|Q\mathcal{H}PG^{(s)-}_P(E)P\mathcal{H}Q|\phi_s\rangle\ . \quad (9)$$

The way of writing Eq. (1) is not unique, depending on the particular ϕ_s state selected to build the Green's operators $G^{(s)}_Q(E)$ and $G^{(s)-}_P(E)$. However, all possible choices provide identical representations of $\psi^-_{\mu E}$, so that, in each particular case, one can single out the ϕ_s state that is more convenient to accelerate convergence in the expansions of the Green's operators. Also, Eq. (1) can be used both in resonant and nonresonant regions.

Then, in order to obtain the continuum state written in Eq. (1) we need to evaluate two kinds of wave functions, ϕ_n and $P\psi^{0-}_{\mu E}$, and their corresponding Green's operators, $G^{(s)}_Q(E)$ and $G^{(s)-}_P(E)$. The ϕ_n wave functions [hence $G^{(s)}_Q(E)$] can be obtained with standard configuration-interaction techniques in the framework of the conventional Feshbach approach [30] or the pseudopotential-Feshbach method [31]. In this paper we will focus on the calculation of $P\psi^{0-}_{\mu E}$ and $G^{(s)-}_P(E)$, which are the non-L^2 integrable parts of the exact eigenfunction $\psi^-_{\mu E}$ in Eq. (1).

Let us define a complete set of orthogonal uncoupled continuum wave functions $\chi^0_{\mu E}$, which are solutions of the single-channel Schrödinger equations:

$$(P_\mu\mathcal{H}P_\mu-E)\chi^0_{\mu E}=0 \quad (10)$$

with

$$P_\mu\chi^0_{\mu E}=\chi^0_{\mu E} \quad (11)$$

and let $\tilde{\chi}^0_{\mu n}$ be the corresponding L^2 representations, which are related to the former representations through a renormalization factor ρ:

$$\chi^0_{\mu E_n}=\rho^{1/2}_\mu(E_n)\tilde{\chi}^0_{\mu n} \ . \tag{12}$$

From these $\tilde{\chi}^0_{\mu n}$ functions, one has two ways to build the correct $P\psi^{0-}_{\mu E}$ state, which we describe below.

A. K-matrix approach

Using the closure relation with the $\tilde{\chi}^0_{\mu n}$ wave functions, one can write the K-matrix scattering equations for a given energy $E=E_n$:

$$\langle\tilde{\chi}^0_{\mu' n'}|K^0|\tilde{\chi}^0_{\mu n}\rangle=\langle\tilde{\chi}^0_{\mu' n'}|V|\tilde{\chi}^0_{\mu n}\rangle+\sum_{\mu''}\sum_{\substack{n'' \\ (E_{n''}\neq E_n)}}\frac{\langle\tilde{\chi}^0_{\mu' n'}|V|\tilde{\chi}^0_{\mu'' n''}\rangle\langle\tilde{\chi}^0_{\mu'' n''}|K^0|\tilde{\chi}^0_{\mu n}\rangle}{E-E_{n''}} \ , \tag{13}$$

where

$$V=\sum_{\substack{\mu\mu' \\ (\mu\neq\mu')}}P_\mu\mathcal{H}P_{\mu'}+P\mathcal{H}QG^{(s)}_Q(E)Q\mathcal{H}P \ . \tag{14}$$

After solution of the K-matrix equations (13), the $P\psi^{0-}_{\mu E}$ wave functions are given by

$$P\psi^{0-}_{\mu E_n}=\sum_\nu(\mathbf{I}-i\pi\mathbf{K}^0)^{-1}_{\mu\nu}\rho^{1/2}_\nu(E_n)\times\left[\tilde{\chi}^0_{\nu n}+\sum_{\mu'}\sum_{n'\neq n}\frac{\langle\tilde{\chi}^0_{\mu' n'}|K^0|\tilde{\chi}^0_{\nu n}\rangle}{E_n-E_{n'}}\tilde{\chi}^0_{\mu' n'}\right] \ , \tag{15}$$

where the $\mathbf{K}^0$ matrix elements are of the form:

$$\langle\chi^0_{\mu' E_{n'}}|K^0|\chi^0_{\mu E_n}\rangle=\rho^{1/2}_{\mu'}(E_{n'})\rho^{1/2}_\mu(E_n)\langle\tilde{\chi}^0_{\mu' n'}|K^0|\tilde{\chi}^0_{\mu n}\rangle \ . \tag{16}$$

The wave function of Eq. (15) is correctly δ normalized and satisfies the asymptotic conditions that are relevant for photoionization problems. In paper I and in Refs. [13,15–17], Eq. (13) was solved iteratively. In this way, convergence can only be achieved if V matrix elements are smaller than energy separations. However, Eq. (13) can be solved in a completely different way by realizing that, for a given channel μ at an energy E_n, it is equivalent to the system of linear equations:

$$\sum_{\mu'',n''}\mathcal{A}_{\mu' n'\mu'' n''}\langle\tilde{\chi}^0_{\mu'' n''}|K^0|\tilde{\chi}^0_{\mu n}\rangle=\mathcal{B}_{\mu' n'} \ , \tag{17}$$

where

$$\mathcal{A}_{\mu' n'\mu'' n''}=\delta_{\mu''\mu'}\delta_{n''n'}+(\delta_{n''n}-1)\frac{\langle\tilde{\chi}^0_{\mu' n'}|V|\tilde{\chi}^0_{\mu'' n''}\rangle}{E_n-E_{n''}} \ , \tag{18}$$

$$\mathcal{B}_{\mu' n'}=\langle\tilde{\chi}^0_{\mu' n'}|V|\tilde{\chi}^0_{\mu n}\rangle \ . \tag{19}$$

We can write a similar system of linear equations for each channel μ. Therefore, simple matrix inversions is all one has to do in order to obtain the K matrix, and this is so irrespective of the strength of the interaction between the zeroth-order uncoupled continua.

In principle, we could also use this method to obtain the corresponding Green's operator $G^{(s)-}_P(E)$ by solving the K-matrix equations for each energy value $E=E_n$. This allows us to write the corresponding spectral resolution of $G^{(s)-}_P(E)$ in the basis of all the $P\psi^{0-}_{\mu E}$ functions. Nevertheless, this is not the simplest way, since the Green's operator can be obtained in a single calculation by using a different point of view.

B. Green's operator method

The $P\psi^{0-}_{\mu E}$ wave function can also be obtained from the Green's operator $G^{(s)-}_P(E)$ associated to the $\mathcal{H}'$ [Eq. (6)] Hamiltonian and the uncoupled states $\chi^0_{\mu E}$:

$$P\psi^{0-}_{\mu E}=\chi^0_{\mu E}+G^{(s)-}_P(E)V\chi^0_{\mu E} \ . \tag{20}$$

From the formal scattering theory we can write

$$G^{(s)-}_P(E)=G^-_0(E)+G^-_0(E)VG^{(s)-}_P(E) \ , \tag{21}$$

where $G^-_0(E)$ is the Green's operator associated to the uncoupled Hamiltonian:

$$G^-_0(E)=\lim_{\eta\to 0}\frac{1}{E-\sum_\mu P_\mu\mathcal{H}P_\mu-i\eta)} \ . \tag{22}$$

In the basis of discretized zeroth-order states the latter operator takes the form

$$\begin{aligned}G^-_0(E_n)&=\sum_{\mu'}\sum_{\substack{n' \\ (E_{n'}\neq E_n)}}\frac{|\tilde{\chi}^0_{\mu' n'}\rangle\langle\tilde{\chi}^0_{\mu' n'}|}{(E_n-E_{n'})}\\&\quad+i\pi\sum_\mu\rho_\mu(E_n)|\tilde{\chi}^0_{\mu n}\rangle\langle\tilde{\chi}^0_{\mu n}|\\&\equiv\sum_{\mu'}\sum_{n'}\Xi_{\mu'}(E_{n'})|\tilde{\chi}^0_{\mu' n'}\rangle\langle\tilde{\chi}^0_{\mu' n'}| \ ,\end{aligned} \tag{23}$$

where

$$\Xi_{\mu'}(E_{n'})=\begin{cases}i\pi\rho_{\mu'}(E_{n'}) & \text{for } E_{n'}=E_n\\ 1/(E_n-E_{n'}) & \text{for } E_{n'}\neq E_n \ .\end{cases} \tag{24}$$

In paper I, we expanded the $G^{(s)-}_P(E)$ operator in a Born series in terms of $G^-_0(E)$, whose discretized representation [Eq. (23)] is very simple. To avoid the intrinsic limitations for the convergence of a Born series, in this work we calculate $G^{(s)-}_P(E)$ by means of Eq. (21), which can be discretized in the following way. Using Eq. (23) and the closure relation in Eq. (21), and projecting from the left and from the right with the $\tilde{\chi}^0_{\mu n}$ functions, we obtain

$$\langle \tilde{\chi}^0_{\mu' n'} | G_P^{(s)-}(E) | \tilde{\chi}^0_{\mu n} \rangle = \delta_{\mu\mu'}\delta_{nn'}\Xi_{\mu'}(E_{n'}) + \Xi_{\mu'}(E_{n'}) \sum_{\mu''} \sum_{n''} \langle \tilde{\chi}^0_{\mu' n'} | V | \tilde{\chi}^0_{\mu'' n''} \rangle \times \langle \tilde{\chi}^0_{\mu'' n''} | G_P^{(s)-}(E) | \tilde{\chi}^0_{\mu n} \rangle , \quad (25)$$

which presents many similarities with Eq. (13). The main difference is that the latter equation involves complex numbers, whereas the K-matrix equations only include real quantities. For a given channel μ, Eq. (25) can also be written in the condensed form

$$\sum_{\mu'',n''} \mathcal{C}_{\mu' n' \mu'' n''} \langle \tilde{\chi}^0_{\mu'' n''} | G_P^{(s)-}(E) | \tilde{\chi}^0_{\mu n} \rangle = \mathcal{D}_{\mu' n'} , \quad (26)$$

where

$$\mathcal{C}_{\mu' n' \mu'' n''} = \delta_{\mu'' \mu'}\delta_{n'' n'} - \Xi_{\mu'}(E_{n'}) \langle \tilde{\chi}^0_{\mu' n'} | V | \tilde{\chi}^0_{\mu'' n''} \rangle , \quad (27)$$

$$\mathcal{D}_{\mu' n'} = \delta_{\mu' \mu}\delta_{n' n}\Xi_{\mu'}(E_{n'}) . \quad (28)$$

Equation (26) represents a system of linear equations in the complex plane for each channel μ. The coefficient matrix **C** multiplying the unknowns is the same for all μ, so that each system of equations differs exclusively in right-hand side column vector **D**. Therefore, only one matrix inversion is required to solve Eq. (26), which means that computer time is independent of the number of channels included in the calculations. The resulting matrix representation of $G_P^{(s)-}(E)$ permits us to evaluate all matrix elements involving $G_P^{(s)-}(E)$ in Eq. (1), as well as the $P\psi^{0-}_{\mu E}$ wave function, whatever the strength of interchannel coupling. We have tested this procedure for the cases considered in paper I: the cross sections provided by solving the systems of Eq. (26) are identical to those of I up to the eight significant figure.

III. PHOTOIONIZATION OF He BETWEEN $N=3$ AND 4

For a two-electron system such as He, the projection operator P can be written [32]

$$P = P_1 + P_2 - P_1 P_2 . \quad (29)$$

As we are interested in photoionization above the $N=3$ threshold, the one-electron operator P_i will be of the form

$$P_i = \sum_{N=1}^{3} \sum_{l=0}^{N-1} \sum_{m=-l}^{l} |\phi_{Nlm}(i)\rangle\langle\phi_{Nlm}(i)| , \quad (30)$$

which includes all hydrogenic ϕ_{Nlm} states of He^+ with $N \leq 3$.

A. Wave functions

The ground-state wave function of helium is the same used in paper I and in Refs. [15–17]. The resonant wave functions ϕ_n have been obtained in the framework of the pseudopotential Feshbach method [31]. The corresponding Hamiltonian has been diagonalized in the basis of 216 configurations built from the Slater-type orbitals (STO's) given in Table I. This basis has been approximately optimized and, as we will see below, leads to an accurate representation of the $4lnl'$ double excited states.

TABLE I. STO basis set used to calculate the eigenfunctions of $Q\mathcal{H}Q$. Each STO is defined as $\varphi(\mathbf{r}) = r^{k-1}\exp(-\alpha r)Y_{lm}(\hat{\mathbf{r}})$.

$l=0$		$l=1$		$l=2$		$l=3$		$l=4$		$l=5$	
k	α	k	α	k	α	k	α	k	α	k	α
1	0.60	2	0.60	3	0.60	4	0.25	5	0.20	6	0.16
2	0.60	3	0.60	3	0.25	5	0.20	6	0.20	7	0.15
1	0.25	2	0.25	4	0.25	6	0.20	7	0.15		
2	0.25	3	0.25	5	0.20	7	0.15	8	0.15		
3	0.25	4	0.25	6	0.20	8	0.15				
4	0.25	5	0.20	7	0.15						
5	0.20	6	0.20	8	0.15						
6	0.20	7	0.15								
7	0.15	8	0.15								
8	0.15										

The nonresonant uncoupled-continuum wave functions $\tilde{\chi}^0_{\mu n}$ have been evaluated in the static exchange approximation, following the standard codes of Macías and coworkers [33]. Briefly, for each channel μ, the uncoupled Hamiltonian $P_\mu \mathcal{H} P_\mu$ is diagonalized in a basis of configurations built from STO's, whose exponents follow an even-tempered sequence; the ensuing discretized eigenfunctions are then renormalized following the recipes of Ref. [33]. The convergence is tested by checking the invariance of the results when the number of STO's is increased.

Finally, the expansion of $G_Q^{(s)}(E)$ in Eq. (5) includes the first 46 eigenfunctions of $Q\mathcal{H}Q$, which represent the $4lnl'$ and $5lnl'$ doubly excited states, and discretized $4l\epsilon l'$ continuum functions that our basis is able to reproduce up to the $N=5$ threshold.

B. Cross sections

The cross sections have been evaluated for photon energies between 73.00 and 75.15 eV. An energy grid with variable step size has been used in order to exhibit the whole resonant structure. We have calculated the partial cross sections for the nine open channels $1s\epsilon p$, $2s\epsilon p$, $2p\epsilon s$, $2p\epsilon d$, $3s\epsilon p$, $3p\epsilon s$, $3p\epsilon d$, $3d\epsilon p$, and $3d\epsilon f$. To gauge the accuracy of the present approach we have compared it with the available experimental results [25–27].

We show in Fig. 1 the $N=1$ cross section, and in Fig. 2 the $N=2$ and 3 ones, in both the length and velocity representations. Gauge invariance is good for $N=2$ and 3. For the $N=1$ cross section, the velocity results are $\sim 5\%$ lower than the length results; however, the corresponding curves have an almost identical shape. This may be explained by the fact that the $1s\epsilon p$ continuum has a strong oscillatory behavior, so that the STO basis used to represent the nonresonant wave function is less complete than for other channels. There are seven series of autoionizing resonances converging to the $N=4$ threshold. Following Herrick and Sinanoglu [20], we will label them with the K and T quantum numbers: (K,T). Only one strong series of resonances is observed: the peaks at 73.71, 74.61, and 74.98 eV, which correspond to the first

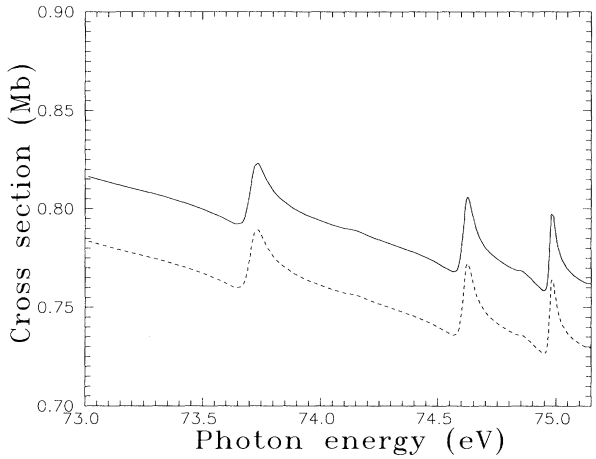

FIG. 1. Partial $\sigma_{N=1}$ photoionization cross section of helium above the $N=3$ threshold. ——, length gauge; — — —, velocity gauge.

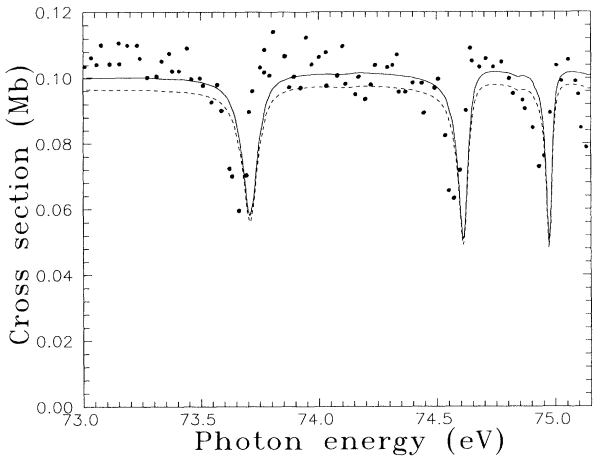

FIG. 3. $\sigma_{N=2}+\sigma_{N=3}$ photoionization cross section of helium above the $N=3$ threshold. ——, length gauge; — — —, velocity gauge; ●, experimental values of Woodruff and Samson [25].

three $4lnl'$ doubly excited states of the (2,1) series. The small features seen at 74.15 and 74.85 eV in Fig. 2 are the first two (0,1) resonances, and the small hump at 74.91 corresponds, probably, to the first resonance of the $(-2,1)$ series.

The results shown in Fig. 2 are close to those of Hayes and Scott [18]; however, there are two significant discrepancies: (i) our resonance positions are shifted to smaller photon energies and (ii) needlelike peaks attributed by these authors to the $(-2,1)$ series of resonances are not seen in the spectra of Fig. 2. In this respect, it must be pointed out that we do obtain such resonances in the diagonalization of $Q\mathcal{H}Q$, but they are not effectively populated by single-photon absorption. In Fig. 2 we have also plotted the experimental results of Heimann *et al.* [26] for the $N=3$ cross section. The agreement between experiment and theory is very good. Woodruff and Samson [25] have measured the $\sigma_{N=2}+\sigma_{N=3}$ cross section in the same energy range. In Fig. 3 we compare the experimental data with the results obtained by adding the two curves of Fig. 2. The overall agreement is good.

In Fig. 4 we have plotted the total photoionization cross section. As for the dominant $1s\epsilon p$ cross section, the length and the velocity results differ by $\sim 5\%$. Very recently, Domke *et al.* [27] have measured, with high-energy resolution, the total photoionization yield in the energy region between 73.2 and 75.5 eV. In this experiment, the cross sections were obtained in arbitrary units. Therefore, in order to compare them, we have subtracted from the length results of Fig. 4 the slow decreasing background, and normalized the experimental cross sections to ours at the first minimum and at the lowest energy. The resulting comparison is displayed in Fig. 5. The use of our velocity data leads to an identical graph. Both

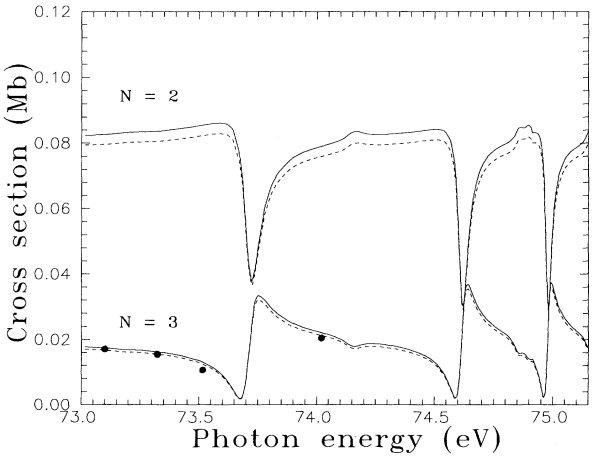

FIG. 2. Partial $\sigma_{N=2}$ and $\sigma_{N=3}$ photoionization cross sections of helium above the $N=3$ threshold. ——, length gauge; — — —, velocity gauge; ●, experimental values of Heimann *et al.* [26].

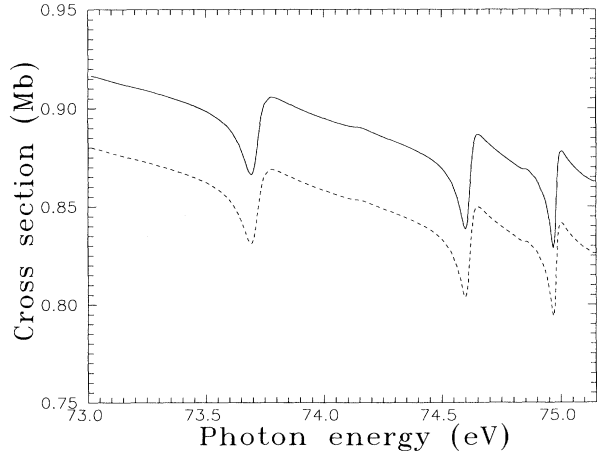

FIG. 4. Total photoionization cross section of helium above the $N=3$ threshold. ——, length gauge; — — —, velocity gauge.

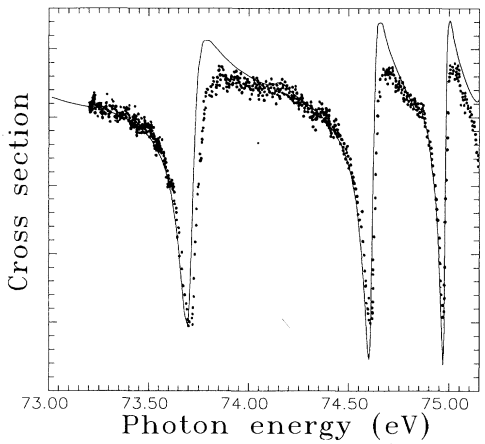

FIG. 5. Total photoionization cross section of helium above the $N=3$ threshold. ——, length gauge; — — —, velocity gauge. The background cross section has been subtracted from the results of Fig. 4; the experimental cross sections ● of Domke *et al.* [27] have been normalized to the theoretical values at the first minimum and at the lowest energy.

energy positions and shapes of the resonance peaks are in very good agreement. In particular, it can be observed that, in this kind of representation, the first (0,1) resonance at 74.15 eV is more clearly exhibited than in Fig. 4 and, in fact, its existence may also be inferred from the experimental data. The excellent agreement found for the energy positions seems to indicate that our description of the doubly excited states with the STO basis of Table I is accurate.

IV. CONCLUSIONS

In this paper we have presented a fully L^2 approach to evaluate continuum wave functions when several strongly interacting channels are open. As in paper I, the method is based on the Feshbach formalism, so that the resonant and nonresonant contributions to the wave function are treated separately. Therefore, specific basis sets can be used to represent each part, thus allowing for a better description of electron correlation.

For the nonresonant part, the continuum wave function can be evaluated either by solving the scattering K-matrix equations or by evaluating the corresponding Green's operator. The K-matrix equations are solved in a representation of discretized uncoupled states, so that for each channel and a given energy, they are equivalent to a system of linear equations.

Alternatively, one can build a representation of the Green's operator in the basis of discretized uncoupled continuum states by using the relation between this Green's operator and a zeroth-order one associated to the uncoupled continua. In this way, for each channel, we are led to a system of linear equations that can be easily solved in the complex plane. In this work, we have used the latter procedure since the coefficient matrix multiplying the unknowns is the same for all channels, which considerably reduces computer time. The ensuing Green's operator permits us not only to obtain the nonresonant wave function, but also to build the continuum eigenstate of $\mathcal{H}$ through Eq. (1).

Unlike paper I, where perturbative expansions were used to solve the scattering equations, the present method can be used with any kind of discretized uncoupled states, provided that they are orthogonal, but irrespective of the interaction strength between them. In particular, in this paper, the discretized uncoupled states have been calculated with a basis of STO's following the standard codes of Macías and co-workers [33].

We have applied the method to study photoionization of helium between the $N=3$ and 4 thresholds, where there are nine open channels. A sample of our results has been presented in order to compare with the few existing experimental measurements [25–28]. Complete information on partial cross sections and resonance parameters will be presented in a forthcoming paper. The calculated cross sections are in good agreement with the experiments, and do not differ essentially from previous calculations [18].

The accuracy that can be reached with the present approach depends directly on the density of zeroth-order discretized states. In this respect, one can increase this accuracy at will by simply increasing the density of continuum states. Therefore, the critical point is to perform accurate discretizations of uncoupled continuum states, for which many different approaches proposed in the literature for a single continuum can be used.

ACKNOWLEDGMENTS

This work has been partially supported by the DGICYT Project No. PB90-213 and the EEC twining Program No. SCI*.0138.C(JR).

[1] J. T. Broad and W. P. Reinhardt, J. Phys. B **9**, 1491 (1976); Phys. Rev. A **14**, 2159 (1976).
[2] B. H. Bransden and A. T. Stelbovics, J. Phys. B **17**, 1877 (1984).
[3] H. A. Slim and A. T. Stelbovics, J. Phys. B **22**, 475 (1989).
[4] R. Lefebvre, J. Phys. Chem. **89**, 4201 (1985).
[5] Y. Sun, M. L. Du, and A. Dalgarno, J. Chem. Phys. **93**, 8840 (1990).
[6] M. L. Du and A. Dalgarno, Phys. Rev. A **43**, 3474 (1991).
[7] G. Jolicard and G. D. Billing, J. Chem. Phys. **97**, 997 (1992).
[8] D. H. Madison and J. Callaway, J. Phys. B **20**, 4197 (1987).
[9] I. Bray, D. A. Konovalov, and I. E. McCarthy, Phys. Rev. A **43**, 1301 (1991).
[10] R. Moccia and P. Spizzo, J. Phys. B **23**, 3557 (1990).
[11] R. Moccia and P. Spizzo, Phys. Rev. A **43**, 2199 (1991).
[12] F. Martín, A. Riera, and I. Sánchez, J. Chem. Phys. **94**, 4275 (1991).
[13] I. Sánchez and F. Martín, Phys. Rev. A **44**, 13 (1991).
[14] I. Sánchez and F. Martín, Phys. Rev. A **44**, 7318 (1991).
[15] I. Sánchez and F. Martín, Phys. Rev. A **45**, 4468 (1992).

[16] I. Sánchez and F. Martín, Phys. Rev. A **47**, 1520 (1993).
[17] I. Sánchez and F. Martín, Phys. Rev. A **47**, 1878 (1993).
[18] M. A. Hayes and M. P. Scott, J. Phys. B **21**, 1499 (1988).
[19] R. S. Oberoi, J. Phys. B **5**, 1120 (1972).
[20] D. R. Herrick and O. Sinanoglu, Phys. Rev. A **11**, 97 (1975).
[21] Y. K. Ho, Phys. Lett. **79A**, 44 (1980).
[22] Y. K. Ho, J. Phys. B **15**, L691 (1982).
[23] Y. Komninos and C. A. Nicolaides, J. Phys. B **19**, 1701 (1986).
[24] O. Robaux, J. Phys. B **20**, 2347 (1987).
[25] P. R. Woodruff and J. A. R. Samson, Phys. Rev. A **25**, 848 (1982).
[26] P. A. Heimann, U. Becker, H. G. Kerkhoff, B. Langer, D. Szostak, R. Wehlitz, D. W. Lindle, T. A. Ferrett, and D. A. Shirley, Phys. Rev. A **34**, 3782 (1986).
[27] M. Domke, C. Xue, A. Puschmann, T. Mandel, E. Hudson, D. A. Shirley, G. Kaindl, C. H. Green, H. R. Sadeghpour, and H. Petersen, Phys. Rev. Lett. **66**, 1306 (1991).
[28] M. Zubek, G. C. King, P. M. Rutter, and F. H. Read, J. Phys. B **22**, 3411 (1989).
[29] H. Feshbach, Ann. Phys. (N.Y.) **19**, 287 (1962).
[30] H. Bachau, J. Phys. B **17**, 1771 (1984).
[31] F. Martín, O. Mó, A. Riera, and M. Yáñez, Europhys. Lett. **4**, 799 (1987); J. Chem. Phys. **87**, 6635 (1987).
[32] Y. Hahn, T. F. O'Malley, and L. Spruch, Phys. Rev. **128**, 932 (1962).
[33] A. Macías, F. Martín, A. Riera, and M. Yáñez, Phys. Rev. A **36**, 4179 (1987); Int. J. Quantum Chem. **33**, 279 (1988).